

# RSC Advances



This is an *Accepted Manuscript*, which has been through the Royal Society of Chemistry peer review process and has been accepted for publication.

*Accepted Manuscripts* are published online shortly after acceptance, before technical editing, formatting and proof reading. Using this free service, authors can make their results available to the community, in citable form, before we publish the edited article. This *Accepted Manuscript* will be replaced by the edited, formatted and paginated article as soon as this is available.

You can find more information about *Accepted Manuscripts* in the [Information for Authors](#).

Please note that technical editing may introduce minor changes to the text and/or graphics, which may alter content. The journal's standard [Terms & Conditions](#) and the [Ethical guidelines](#) still apply. In no event shall the Royal Society of Chemistry be held responsible for any errors or omissions in this *Accepted Manuscript* or any consequences arising from the use of any information it contains.

**A CdTe/CdS/ZnS core/shell/shell QDs-based “OFF-ON”  
fluorescent biosensor for sensitive and specific determination  
of L-ascorbic acid**

**Shan Huang<sup>a,b</sup>, Fawei Zhu<sup>a</sup>, Qi Xiao<sup>a,b,c,\*</sup>, Wei Su<sup>a</sup>, Jiarong Sheng<sup>a</sup>, Chusheng  
Huang<sup>a</sup> and Baoqing Hu<sup>b</sup>**

<sup>a</sup> *College of Chemistry and Life Science, Guangxi Teachers Education University, Nanning 530001, P. R. China*

<sup>b</sup> *Key Laboratory of Beibu Gulf Environment Change and Resources Utilization (Guangxi Teachers Education University), Ministry of Education, P. R. China*

<sup>c</sup> *State Key Laboratory of Virology, Wuhan University, P. R. China*

\* Corresponding author. Tel.: +86 771 3908065; Fax: +86 771 3908065;  
E-mail address: [qi.xiao@whu.edu.cn](mailto:qi.xiao@whu.edu.cn)

**Abstract:** We report here a quantum dots (QDs)-based “OFF-ON” fluorescent biosensor for sensitive and specific determination of L-ascorbic acid. The proposed one-pot L-ascorbic acid detection method is quite simple, rapid and convenient due to the elimination of the modification and separation procedures. In this contribution, the *N*-acetyl-L-cysteine (NAC)-capped CdTe/CdS/ZnS core/shell/shell QDs were synthesized in aqueous phase. Subsequently, KMnO<sub>4</sub> was added into solution and attached to QDs surface to effectively quench the fluorescence of QDs, which rendered QDs into fluorescence “OFF” status. After the addition of L-ascorbic acid into the QDs–KMnO<sub>4</sub> system, the fluorescence of QDs could then be “ON”, because L-ascorbic acid could bind with KMnO<sub>4</sub> and break KMnO<sub>4</sub> away from the surface of QDs. Under the optimized conditions, the relative restored fluorescence intensity was directly proportional to the concentration of L-ascorbic acid in the range of  $8.0 \times 10^{-9}$  M ~  $1.0 \times 10^{-7}$  M, with a correlation coefficient of 0.9971 and a limit of detection of  $1.8 \times 10^{-9}$  M. The relative standard deviation for  $6.0 \times 10^{-8}$  M L-ascorbic acid was 2.1% (n = 5). There was almost no interference to some common ions, carbohydrates, nucleotides and amino acids. The proposed method was applied to the determination of L-ascorbic acid in three synthetic samples, human urine samples and vitamins C tablets with satisfactory results. The possible fluorescence quenching mechanism of this fluorescent sensor was further investigated by UV–Vis spectroscopy.

**Keywords:** CdTe/CdS/ZnS core/shell/shell quantum dots; Fluorescent biosensor; L-Ascorbic acid; Determination

## 1. Introduction

Due to the specific optical properties dramatically different from those in bulk semiconductors, the water-soluble semiconductor quantum dots (QDs) have attracted great attentions as novel fluorescent biosensor in the past two decades.<sup>1-5</sup> Some bio-related small molecules, nucleic acids, proteins and enzymes have been detected by using the fluorescent QDs as the probe based on the fluorescence quenching or the fluorescence enhancement of QDs.<sup>6-10</sup> However, both the fluorescence quenching and the fluorescence enhancement of QDs belong to the unidirectional fluorescence variations of QDs, which make this fluorescent QDs biosensor are quite liable to be affected by foreign substances. Hence, it is much more urgent to explore new strategies to increase the selectivity and expand the bio-applications of fluorescent QDs biosensors.

Recently, the fluorescence “OFF-ON” sensors based on QDs have been explored and realized simple and sensitive determination of some chemical substances.<sup>11-13</sup> In addition, this fluorescence “OFF-ON” mode has been used to detect some bio-related small molecules and biomacromolecules.<sup>14-22</sup> Zhu and co-workers demonstrated an “OFF-ON” approach for detection of both  $\text{Cu}^{2+}$  and L-cysteine by using fluorescent carbon dots probes.<sup>14</sup> Yi et al. reported a dual-mode nanosensor with both colorimetric and fluorometric readout based on carbon QDs and gold nanoparticles for specific detection of glutathione.<sup>15</sup> Su’s group established a novel fluorescence “TURN OFF-ON” nanosensor for the determination of heparin and heparinase based on  $\text{CuInS}_2$  QDs.<sup>16</sup> Renganathan et al. described a novel platform for detecting double stranded DNA (dsDNA) by tracing the “ON-OFF-ON” fluorescence signals of QDs–porphyrin system.<sup>17</sup> Xie et al. proposed a new dsDNA detection method relying on the single-color fluorescence “OFF-ON” switch system that was composed of CdTe QDs and  $\text{Ru}(\text{phen})_2(\text{dppz})^{2+}$ .<sup>18</sup> He and her co-workers also applied this QDs-based fluorescence “OFF-ON” model to detect both anticancer drugs and dsDNA.<sup>21,22</sup> Because of the high selectivity and high sensitivity, this novel QDs-based “OFF-ON” fluorescent sensor showed great potential applications in biochemical and biomedical determinations.

It is well-known that L-ascorbic acid is a hexanoic sugar acid with a  $\gamma$ -lactone structure and two dissociable protons ( $\text{p}K_a$  4.04 and 11.34), so L-ascorbic acid occurs as an ascorbate anion under the physiological conditions. Due to the high reductive properties, L-ascorbic acid is largely used

as a powerful antioxidant in free-radical induced diseases therapy, since L-ascorbic acid can easily balance the oxidative stress of human body.<sup>23,24</sup> In addition, L-ascorbic acid can take crucial part in some biochemical processes and can also serve as an effect drugs for some diseases.<sup>25,26</sup> However, the excess of L-ascorbic acid can lead to taste/aroma deterioration, diarrhea, kidney calculi and gastric irritation.<sup>27</sup> Because of the important role of L-ascorbic acid in biochemistry and biomedical applications, the detection of L-ascorbic acid becomes more important and attracts considerable interest in recent years. Until now, various analytical techniques have been reported for the detection of L-ascorbic acid in biological and pharmaceutical samples, such as spectrophotometry,<sup>28</sup> enzymatic analysis,<sup>29</sup> electroanalysis,<sup>30</sup> chemiluminescence<sup>31</sup>, colorimetry<sup>32-34</sup>, phosphorimetry<sup>35</sup> and liquid chromatography.<sup>36</sup> But some of these methods are time-consuming, complicated and expensive cost to certain extent. Thus, there is an urgent demand for simple and rapid biosensor for L-ascorbic acid with high sensitivity and specificity in clinical analysis and pharmaceutical industry. Recent years, fluorescence analysis has been widely utilized for L-ascorbic acid determination due to their unique advantages of simplicity, rapidity, high sensitivity and low cost of instrumentation and maintenance. Yan and co-workers reported a CdTe QDs-based turn-on fluorescent sensor for L-ascorbic acid detection.<sup>37</sup> This approach avoids the complicated modification process of QDs, and opens a simple strategy to develop cost-effective, sensitive and selective QD-based fluorescence turn-on sensor for biologically significant antioxidants.

In the present study, the *N*-acetyl-L-cysteine (NAC)-capped CdTe/CdS/ZnS core/shell/shell QDs were synthesized in aqueous phase.<sup>38</sup> Since the ligand NAC is water-solubility, environmentally friendly and possesses good biocompatibility, the as-synthesized NAC-capped CdTe/CdS/ZnS core/shell/shell QDs are of crucial importance for many biomedical applications. Herein, we establish a sensitive and specific NAC-capped CdTe/CdS/ZnS core/shell/shell QDs-based “OFF-ON” fluorescent biosensor for L-ascorbic acid by utilizing KMnO<sub>4</sub> as both the quencher to QDs and the oxidizing/binding agent to L-ascorbic acid (Scheme 1). Since KMnO<sub>4</sub> can attach to the surface of QDs and subsequently quench the fluorescence of QDs through the electron transfer process, QDs become to be the fluorescence “OFF” status. After the addition of L-ascorbic acid, KMnO<sub>4</sub> can react and combine with L-ascorbic acid through redox reaction and coordination reaction,<sup>39</sup> and then the electron transfer from QDs to KMnO<sub>4</sub> is interrupted and the

fluorescence of QDs can be “ON” again. This QDs-based “OFF-ON” fluorescent biosensor can be used to detect L-ascorbic acid with the properties of simplicity, sensitivity and specificity. Furthermore, the QDs-based “OFF-ON” fluorescent biosensor has been successfully applied to the detection of L-ascorbic acid in three synthetic samples, human urine samples and vitamins C tablets with satisfactory results.

<Scheme 1>

## 2. Materials and methods

### 2.1. Materials

Te powder (200 meshes, 99.8%), NaBH<sub>4</sub> (99.8%), CdCl<sub>2</sub>·H<sub>2</sub>O (99.99%), NAC (≥ 99%), rhodamine 6G were purchased from Sigma (St. Louis, MO, USA). Na<sub>2</sub>S, ZnCl<sub>2</sub>, 2-propanol, KMnO<sub>4</sub>, L-ascorbic acid, lactose, sucrose, glucose, four nucleotide acids and twenty amino acids were obtained from Sinopharm Chemical Reagent Factory (Shanghai, China). All other reagents were of analytical-reagent grade and used as received. Ultrapure water with a resistivity of 18.2 MΩ cm was produced by passing through a RiOs 8 unit followed by a Millipore-Q Academic purification set (Millipore, Bedford, MA, USA) and used throughout the whole experiments.

### 2.2. Apparatus

The absorption spectra were measured on TU-1901 UV-Vis spectrophotometer (Beijing Purkinje General Instrument Co., Ltd., Beijing, China). All fluorescence spectra and intensities were recorded with Perkin-Elmer Model LS-55 luminescence spectrometer (PerkinElmer, Waltham, MA, USA) equipped with a 20KW xenon discharge lamp as light source. Quartz cells (1 cm path-length) were used for all measurements. All pH measurements were made with a basic pH meter PB-10 (Sartorius Scientific Instruments Co., Ltd., Beijing, China).

### 2.3. Preparations of NAC-capped CdTe/CdS/ZnS core/shell/shell QDs

NAC-capped CdTe/CdS/ZnS core/shell/shell QDs were synthesized according to the method we reported previously.<sup>38</sup> Briefly, 0.2 mmol of Te powder and 1.0 mmol of NaBH<sub>4</sub> were put into a two-necked flask equipped with a constant pressure funnel containing 5.0 mL of ultrapure water. Then the air was pumped off and replaced by nitrogen. After that, the mixture was heated to 80 °C

and lasted for 30 min under nitrogen protection until solution became dark red. The obtained NaHTe solution was stored under nitrogen protection for further use at room temperature. Then, 0.2 mmol of CdCl<sub>2</sub> and 0.34 mmol of NAC solution were mixed in a 40 mL solution and the pH of the mixture was adjusted to 12.0 by dropwise adding 1.0 M NaOH solution under stirring. Then the mixture was transferred into a three-necked flask and the air in the system was replaced with nitrogen. Under stirring, 1 mL of NaHTe solution (0.04 mmol) was added into the Cd precursor solution by syringe at room temperature, which made the molar ratio of Cd : Te : NAC was fixed at 1.0 : 0.2 : 1.7. Then the mixture was heated to 100 °C and reacted at this temperature for 8 min. After that, heat was removed immediately and the mixture was cooled down to room temperature. In order to remove the excess NAC-Cd complexes at the end of the synthesis, cold 2-propanol was added to the reaction mixture to precipitate CdTe core QDs. The as-prepared precipitate was redispersed in ultrapure water.

The CdTe/CdS precursor solution was prepared by adding the as-prepared NAC-capped CdTe core QDs to a nitrogen-saturated solution containing 1.0 mmol CdCl<sub>2</sub>, 0.2 mmol Na<sub>2</sub>S and 5.0 mmol NAC. The CdTe/CdS precursor solution (40 mL) was placed in a three-necked flask. The air in the system was pumped off and replaced with nitrogen. Then the mixture was heated to 100 °C and reacted at this temperature for 15 min. NAC-capped CdTe/CdS core/shell QD samples were taken when the temperature had cooled down to room temperature. Cold 2-propanol was added to precipitate the NAC-capped CdTe/CdS core/shell QDs and the as-prepared precipitate were redispersed in ultrapure water.

The CdTe/CdS/ZnS precursor solution was prepared by adding the as-prepared NAC-capped CdTe/CdS core/shell QDs to a nitrogen-saturated solution containing 1.0 mmol ZnCl<sub>2</sub>, 0.2 mmol Na<sub>2</sub>S and 5.0 mmol NAC. The CdTe/CdS/ZnS precursor solution (40 mL) was placed in a three-necked flask. The air in the system was pumped off and replaced with nitrogen. Then the mixture was heated to 70 °C and reacted at this temperature for 10 min. NAC-capped CdTe/CdS/ZnS core/shell/shell QD samples were taken when the temperature had cooled down to room temperature. Cold 2-propanol was added to precipitate NAC-capped CdTe/CdS/ZnS core/shell/shell QDs, which were dried overnight under vacuum at 30 °C and stored in a refrigerator for further experiments. The concentration of the water-soluble NAC-capped CdTe/CdS/ZnS core/shell/shell QDs was estimated from the absorption spectra using the molar

absorptivity at the first absorption maximum for QDs reported by Peng and co-workers.<sup>36</sup>

#### 2.4. Preparation of three synthesis samples and human urine samples

For synthetic samples detection, three samples were prepared by mixing the standard solution of different solution with different concentrations in the reaction system. Sample 1 contained twenty amino acids and their concentration were all  $1.0 \times 10^{-5}$  M. Glucose, sucrose, lactose and urea in sample 2 were all  $2.0 \times 10^{-4}$  M. Adenine, cytosine, thymine and guanine in sample 2 were all  $1.0 \times 10^{-5}$  M. The concentrations of  $\text{KNO}_3$ ,  $\text{NaNO}_3$ ,  $\text{Ca}(\text{C}_2\text{O}_4)_2$ ,  $\text{Mg}(\text{NO}_3)_2$ ,  $\text{Al}(\text{NO}_3)_3$ ,  $\text{CuSO}_4$  in sample 3 were all  $1.0 \times 10^{-4}$  M. Different amounts of L-ascorbic acid standard solution were added into the reaction system and the final concentration of L-ascorbic acid was  $1.5 \times 10^{-7}$  M in sample 1,  $5.0 \times 10^{-7}$  M in sample 2 and  $8.0 \times 10^{-7}$  M in sample 3, respectively. The recovery of L-ascorbic acid in three synthetic samples was examined by the proposed method.

Human urine samples were obtained from five healthy volunteers (two woman and three men, age range 25 ~ 35 years) and prepared as reported before.<sup>6</sup> Each of 500  $\mu\text{L}$  fresh samples was taken and combined with 1 mL solutions (containing 4.0 mM  $\text{Na}_2\text{EDTA}_4$  and 2.0 M  $\text{HClO}_4$ ) in a 2 mL eppendorf tube, causing the proteins to separate. After standing for 30 min to precipitate proteins, the sample was centrifuged for 15 min at 4500 rpm. The supernatant liquid of 500  $\mu\text{L}$  was adjusted to pH 7.8 by NaOH solution and then diluted to 2 mL with 0.01 M pH 7.8 PB. After homogenizing, the sample was filtered with 0.22  $\mu\text{m}$  Millipore membranes (Millipore, Bedford, MA, USA). The filtrate was collected and stored at 4  $^\circ\text{C}$  (three days) until fluorescence analysis. Human urine samples were diluted 1000-fold with ultrapure water before analysis.<sup>35</sup>

Vitamins C tablets were produced by Shanghai Quanyu Biological Technology Suiping Pharmaceutical Co., Ltd. (Suiping, China). The content of L-ascorbic acid in each vitamins C tablet is about 0.1 g. 5 pieces of vitamins C tablets were mixed and powdered in a mortar. The weight of vitamins C tablets was weighed and the average weight of each tablet was calculated to be 0.12 g. 0.06 g powder was weighed and dissolved in 10 mL ultrapure water. The solution was filtrated with 0.22  $\mu\text{m}$  Millipore filter to remove the insoluble components. After that, the filtrate was transferred into 250 mL volumetric flask and diluted to 250 mL with ultrapure water. The pre-treated vitamins C tablet solution was stored in dark at 4  $^\circ\text{C}$  and was diluted 5000-fold with ultrapure water before analysis.

## 2.5. L-Ascorbic acid detection

As depicted in Scheme 1, firstly, 50  $\mu\text{L}$   $1.0 \times 10^{-5}$  M of NAC-capped CdTe/CdS/ZnS core/shell/shell QDs, 1.5 mL Tris-HCl (pH 7.4) and the appropriate aliquot of  $\text{KMnO}_4$  solution were transferred into a 5 mL eppendorf tube. The mixture was stirred thoroughly and finally diluted to 5 mL with ultrapure water. After 5 min reaction at room temperature, the fluorescence spectra were measured for the selection of the appropriate  $\text{KMnO}_4$  concentration.

For L-ascorbic acid detection, 50  $\mu\text{L}$   $1.0 \times 10^{-5}$  M of NAC-capped CdTe/CdS/ZnS core/shell/shell QDs, 1.5 mL Tris-HCl (pH 7.4) and 30  $\mu\text{L}$   $3.0 \times 10^{-4}$  M of  $\text{KMnO}_4$  solution were transferred into a 5 mL eppendorf tube and the mixture was stirred thoroughly. After incubation for 5 min, the appropriate aliquot of L-ascorbic acid solution were added into the mixture and finally diluted to 3 mL with ultrapure water. After additional 15 min incubation at room temperature, the fluorescence spectra were measured for the quantitative analysis of L-ascorbic acid. When samples were determined, the L-ascorbic acid standard solution was substituted by the prepared sample solution described in Section 2.4.

The fluorescence spectra were recorded at excitation wavelength of 388 nm and the band-slits of excitation and emission were set as 10.0 nm and 10.0 nm, respectively. The fluorescence spectra were recorded from 535 nm to 725 nm, the fluorescence intensity of NAC-capped CdTe/CdS/ZnS core/shell/shell QDs at 622 nm was used for quantitative analysis of L-ascorbic acid.

## 3. Results and discussion

### 3.1. Properties of NAC-capped CdTe/CdS/ZnS core/shell/shell QDs

The normalized UV-Vis absorption and fluorescence spectra of NAC-capped CdTe/CdS/ZnS core/shell/shell QDs at room temperature are shown in Fig. 1. As shown in Fig. 1, the first absorption maximum wavelength of NAC-capped CdTe/CdS/ZnS core/shell/shell QDs was at 578 nm (Fig. 1a), and the particle sizes of these QDs were calculated to be about 3.5 nm according to the first absorption maximum wavelength of QDs.<sup>40</sup> It could be seen from Fig. 1b that these NAC-capped CdTe/CdS/ZnS core/shell/shell QDs exhibited obvious and symmetrical fluorescent spectrum without a tail on the right-hand side, and the emission maximum wavelength of these

QDs was at 622 nm when the excitation wavelength was chosen at 388 nm. The line width of the fluorescence spectrum of these NAC-capped CdTe/CdS/ZnS core/shell/shell QDs was narrow, indicating that the as-prepared QDs were nearly monodisperse and homogeneous. The fluorescence quantum yield of these QDs was calculated to be about 42% by using rhodamine 6G as fluorescence standard according to the reference reported before.<sup>41</sup>

<Fig. 1>

### 3.2. Characterization of QDs-based fluorescence “OFF-ON” mode

The fluorescence of NAC-capped CdTe/CdS/ZnS core/shell/shell QDs can be quenched effectively by  $\text{KMnO}_4$ , which render QDs into fluorescence “OFF” status. The fluorescence spectra of NAC-capped CdTe/CdS/ZnS core/shell/shell QDs with different concentrations of  $\text{KMnO}_4$  are shown in Fig. 2. It could be seen from Fig. 2A that the fluorescence of NAC-capped CdTe/CdS/ZnS core/shell/shell QDs was seriously quenched after the addition of  $\text{KMnO}_4$ . Since  $1.7 \times 10^{-6}$  M,  $2.3 \times 10^{-6}$  M and  $3.0 \times 10^{-6}$  M for  $\text{KMnO}_4$  presented a quenching effect of 26%, 51% and 93%, respectively, it could also be deduced easily that the fluorescence quenching effect for the NAC-capped CdTe/CdS/ZnS core/shell/shell QDs– $\text{KMnO}_4$  system was mainly the concentration dependent. Furthermore, the fluorescence peaks of the NAC-capped CdTe/CdS/ZnS core/shell/shell QDs– $\text{KMnO}_4$  system were still at 622 nm without any shift, which confirmed the inferred electron transfer mechanism between NAC-capped CdTe/CdS/ZnS core/shell/shell QDs and  $\text{KMnO}_4$ .

<Fig. 2>

The fluorescence of NAC-capped CdTe/CdS/ZnS core/shell/shell QDs could be “ON” after the addition of L-ascorbic acid into the QDs– $\text{KMnO}_4$  system. The fluorescence spectra of NAC-capped CdTe/CdS/ZnS core/shell/shell QDs– $\text{KMnO}_4$  system with different concentrations of L-ascorbic acid are shown in Fig. 2B. According to Fig. 2B, the fluorescence intensity of NAC-capped CdTe/CdS/ZnS core/shell/shell QDs was restored gradually with the increasing of the concentration of L-ascorbic acid. Since the fluorescence restoring effect was mainly the L-ascorbic acid concentration dependent,  $8.0 \times 10^{-8}$  M,  $5.0 \times 10^{-7}$  M and  $1.0 \times 10^{-6}$  M for L-ascorbic acid presented a restoring effect of 16%, 36% and 58%, respectively, the fluorescence restoration approach could be used for the sensitive detection of L-ascorbic acid. Furthermore, the

fluorescence intensity of NAC-capped CdTe/CdS/ZnS core/shell/shell QDs was almost not affected by  $1.0 \times 10^{-6}$  M L-ascorbic acid, validating the specific interaction between  $\text{KMnO}_4$  and L-ascorbic acid that resulted in the fluorescence “ON” status of QDs.

### 3.3. Effect of reaction time

The effect of reaction time on the fluorescence quenching of NAC-capped CdTe/CdS/ZnS core/shell/shell QDs by  $\text{KMnO}_4$  was investigated. Preliminary experiments demonstrated that the fluorescence quenching of NAC-capped CdTe/CdS/ZnS core/shell/shell QDs by  $\text{KMnO}_4$  was finished within 3 min and the fluorescence signals remained constant for more than 60 min, indicating that the NAC-capped CdTe/CdS/ZnS core/shell/shell QDs– $\text{KMnO}_4$  system exhibited good stability. So, the fluorescence intensity of NAC-capped CdTe/CdS/ZnS core/shell/shell QDs– $\text{KMnO}_4$  system was recorded after the addition of  $\text{KMnO}_4$  for 5 min.

The effect of reaction time on the fluorescence of NAC-capped CdTe/CdS/ZnS core/shell/shell QDs– $\text{KMnO}_4$  system by L-ascorbic acid was also studied. The results indicated that the fluorescence restoration of NAC-capped CdTe/CdS/ZnS core/shell/shell QDs by L-ascorbic acid was finished within 10 min and lasted for more than 90 min, which indicated that the NAC-capped CdTe/CdS/ZnS core/shell/shell QDs– $\text{KMnO}_4$ –L-ascorbic acid system exhibited higher stability. Therefore, the fluorescence intensity of NAC-capped CdTe/CdS/ZnS core/shell/shell QDs– $\text{KMnO}_4$ –L-ascorbic acid system was measured after adding L-ascorbic acid for 15 min.

### 3.4. Influence of pH value and buffer volume

Since the pH value of the solution played a quite important role in the interaction of QDs with other molecules,<sup>6,42</sup> the influence of different pH values on the fluorescence intensity reflecting the interaction of both NAC-capped CdTe/CdS/ZnS core/shell/shell QDs with  $\text{KMnO}_4$  and NAC-capped CdTe/CdS/ZnS core/shell/shell QDs– $\text{KMnO}_4$  system with L-ascorbic acid was investigated from pH 6.5 to 10.0. The variation in fluorescence intensities between QDs– $\text{KMnO}_4$  system and QDs– $\text{KMnO}_4$ –L-ascorbic acid system was shown in Fig. 3A. It was found that the change of fluorescence intensity increased gradually with the increment of pH value from 6.5 to 7.4. When pH value was higher than 7.4, the change of fluorescence intensity decreased dramatically. The maximum change of fluorescence intensities occurred when pH value was 7.4.

Therefore, Tris-HCl buffer with pH 7.4 was chosen for further experiments.

Simultaneously, the impact of the volume of Tris-HCl buffer on the fluorescence intensities between NAC-capped CdTe/CdS/ZnS core/shell/shell QDs–KMnO<sub>4</sub> system and NAC-capped CdTe/CdS/ZnS core/shell/shell QDs–KMnO<sub>4</sub>–L-ascorbic acid system was also investigated. As shown in Fig. 3B, the change of fluorescence intensity increased gradually with the increment of Tris-HCl buffer volume from 0 to 1.5 mL. When the volume of Tris-HCl buffer was higher than 1.5 mL, the change of fluorescence intensity decreased gradually. The results indicated that the maximum change of fluorescence intensities occurred when the volume of Tris-HCl buffer was 1.5 mL, so 1.5 mL Tris-HCl buffer was selected as the reaction medium.

<Fig. 3>

### 3.5. Influence of QDs volume

The influence of NAC-capped CdTe/CdS/ZnS core/shell/shell QDs volume on the fluorescence “OFF-ON” systems was also tested. The results of the previous experiment indicated that the quench efficiency of the fluorescence intensity of QDs by KMnO<sub>4</sub> increased obviously when the volume of QDs was in the range of 10 ~ 50 μL. The quench efficiency decreased gradually when the volume of QDs was higher than 50 μL, because higher QDs volume would disturb the electrostatic balance of QDs themselves and affect the electron transfer process from QDs to KMnO<sub>4</sub>. Since the maximum change of the fluorescence intensities between NAC-capped CdTe/CdS/ZnS core/shell/shell QDs and NAC-capped CdTe/CdS/ZnS core/shell/shell QDs–KMnO<sub>4</sub> system appeared when the volume of QDs was 50 μL (Fig. 3C), 50 μL of NAC-capped CdTe/CdS/ZnS core/shell/shell QDs was chosen in this study.

### 3.6. Influence of KMnO<sub>4</sub> concentration

In order to improve the sensitivity of this NAC-capped CdTe/CdS/ZnS core/shell/shell QDs-based “OFF-ON” fluorescent biosensor, the concentration of the quencher becomes much important and should be investigated. As shown in Fig. 4, KMnO<sub>4</sub> could quench the fluorescence of QDs efficiently and the fluorescence quenching effect of the NAC-capped CdTe/CdS/ZnS core/shell/shell CdTe QDs–KMnO<sub>4</sub> system was mainly concentration dependent. The fluorescence intensity quenching of NAC-capped CdTe/CdS/ZnS core/shell/shell CdTe QDs was proportional

to the concentration of  $\text{KMnO}_4$  in the range of  $2.0 \times 10^{-8} \text{ M} \sim 1.7 \times 10^{-6} \text{ M}$ , which could be described by the Stern-Volmer equation:<sup>43</sup>

$$\frac{I_0}{I} = 1 + K_{\text{SV}}[Q]$$

Herein,  $I_0$  and  $I$  are the fluorescence intensities of QDs in the absent and present of  $\text{KMnO}_4$ , respectively.  $K_{\text{SV}}$  represents the Stern-Volmer quenching constant and  $[Q]$  represents the concentration of  $\text{KMnO}_4$ , respectively. As shown in the insert in Fig. 4, the linear regression equation was  $I_0/I - 1 = 0.19 \times [\text{KMnO}_4]$  and the  $K_{\text{SV}}$  value of  $\text{KMnO}_4$  was  $1.9 \times 10^5 \text{ M}^{-1}$ .

<Fig. 4>

In order to provide an optimal “OFF” state of the biosensor, higher concentration of quencher should be applied to the turnoff of the fluorescence of QDs completely. But on the other hand, too much quencher in the system will hamper the response sensitivity of subsequent L-ascorbic acid detection. According to the preliminary experimental results, when the concentration of  $\text{KMnO}_4$  was chosen at  $3.0 \times 10^{-6} \text{ M}$ , a tiny concentration of L-ascorbic acid ( $8.0 \times 10^{-9} \text{ M}$ ) could restore the fluorescence intensity of NAC-capped CdTe/CdS/ZnS core/shell/shell QDs effectively. So,  $3.0 \times 10^{-6} \text{ M}$   $\text{KMnO}_4$  was employed to be the quencher of the NAC-capped CdTe/CdS/ZnS core/shell/shell QDs in the biosensor preparation.

### 3.7. Detection of L-ascorbic acid

The fluorescence of NAC-capped CdTe/CdS/ZnS core/shell/shell QDs could be “ON” after the addition of L-ascorbic acid into the NAC-capped CdTe/CdS/ZnS core/shell/shell QDs– $\text{KMnO}_4$  system. The fluorescence spectra of NAC-capped CdTe/CdS/ZnS core/shell/shell QDs– $\text{KMnO}_4$  system with different concentration of L-ascorbic acid are shown in Fig. 5. Under the optimum conditions, the fluorescence intensity restoration of NAC-capped CdTe/CdS/ZnS core/shell/shell QDs– $\text{KMnO}_4$  system was proportional to the concentration of L-ascorbic acid in the range of  $8.0 \times 10^{-9} \text{ M} \sim 1.0 \times 10^{-7} \text{ M}$  with a correlation coefficient of 0.9971. The linear relationship between the change of fluorescence intensity of NAC-capped CdTe/CdS/ZnS core/shell/shell QDs and L-ascorbic acid concentration in that range was also shown in the insert of Fig. 5. The linear regression equation was  $I - I_0 = 0.91 \times [\text{L-ascorbic acid}]$ . The relative standard deviation for  $6.0 \times 10^{-8} \text{ M}$  L-ascorbic acid was 2.1% ( $n = 5$ ). Based on the three times standard deviation of 12 measurements of NAC-capped CdTe/CdS/ZnS core/shell/shell QDs– $\text{KMnO}_4$  system alone, the

limit of detection for L-ascorbic acid was up to  $1.8 \times 10^{-9}$  M which could be comparable to the most sensitive methods reported for L-ascorbic acid detection (Table 1).

<Fig. 5>

<Table 1>

### 3.8. Effect of foreign substances and sample determination

The influence of some common ions, carbohydrates, nucleotides and amino acids is investigated to verify the applicability of this NAC-capped CdTe/CdS/ZnS core/shell/shell QDs-based “OFF-ON” fluorescent biosensor for L-ascorbic acid determinations in biological samples, and the results are shown in Table 2. The coexisting compounds are considered to have no interference with the detection if they cause a relative error of less than  $\pm 5\%$  in the fluorescence intensity of the system. As shown in Table 2, most common ions, carbohydrates, four nucleotides and twenty amino acids with higher concentration had almost no distinct influence on the determination of  $3.0 \times 10^{-7}$  M L-ascorbic acid in the given conditions. The data revealed that the proposed method might be applied to the detection of L-ascorbic acid in biological samples.

<Table 2>

To confirm the feasibility, this present method was firstly applied to the detection of L-ascorbic acid in three synthetic samples which contained four common chemical substances, three carbohydrates, four nucleotides and twenty amino acids. As indicated in Table 3, the values found for the three synthetic samples were identical with the expected values and the recoveries were from 98.9% to 101.3%, which indicated the suitability of the determination of L-ascorbic acid in the present of these substances.

<Table 3>

To further confirm the feasibility for L-ascorbic acid assay in biological conditions, this method was applied to the determination of L-ascorbic acid in human urine samples. The urine of individuals was treated as described in Section 2.4 and their L-ascorbic acid concentrations were measured according to the proposed method. The recovery of L-ascorbic acid was determined by comparing the results obtained before and after the addition of standard L-ascorbic acid to the diluted uric samples. As listed in Table 4, the recoveries of different known amounts of L-ascorbic acid took were obtained from 95.6% to 104.5% with a satisfying analytical precision ( $R.S.D. \leq$

3.6%), validating the reliability and practicality of this method. In addition, this present approach was applied to L-ascorbic acid detection in vitamins C tablet. As indicated in Table 5, the value found for the sample was highly identical with the expected values, and the recoveries of spiked L-ascorbic acid were obtained from 95.5% to 103.1% with a satisfying analytical precision (R.S.D.  $\leq 3.0\%$ ), which validated the reliability and practicality of this strategy.

<Table 4>

<Table 5>

### 3.9. Possible fluorescence quenching mechanism

It is widely reported that the fluorescence quenching mechanism usually includes the inner filter effect (IFE), non-radiative ground state complex formation (static quenching) and electron transfer processes (dynamic quenching) and so on.<sup>44</sup> Well, the IFE quenching mechanism could be proved through the UV-Vis absorption spectrum of  $\text{KMnO}_4$  and the emission spectrum of NAC-capped CdTe/CdS/ZnS core/shell/shell QDs. As shown in Fig. 6A, the absorption spectrum of  $\text{KMnO}_4$  had three typical absorption bands at 506 nm, 525 nm and 545 nm, respectively; however, the emission peak of NAC-capped CdTe/CdS/ZnS core/shell/shell QDs was centered at 622 nm under the excitation of 388 nm. So, almost no spectral overlap took place between the absorption spectrum of  $\text{KMnO}_4$  and the emission spectrum of NAC-capped CdTe/CdS/ZnS core/shell/shell QDs. Furthermore, the absorbance of  $\text{KMnO}_4$  at 388 nm was also very weak. Therefore,  $\text{KMnO}_4$  could not shield the excitation light for QDs efficiently and neither absorb the emission light from QDs effectively, suggesting that the quenching mechanism between  $\text{KMnO}_4$  and NAC-capped CdTe/CdS/ZnS core/shell/shell QDs was not IFE.<sup>45,46</sup>

<Fig. 6>

Charge transfer is often occurred in the dynamic quenching and fluorescence is quenched subsequently when the electron acceptor collides with the excited fluorophore, so no variations in the absorption spectra of fluorophore will be expected. However, the ground state complex formation during the state quenching can perturb the absorption spectra of fluorophore, which results in the variation of the absorption spectra of fluorophore.<sup>47</sup> In order to precisely reveal the fluorescence quenching mechanism, the UV-Vis absorption spectra of NAC-capped CdTe/CdS/ZnS core/shell/shell QDs,  $\text{KMnO}_4$  and NAC-capped CdTe/CdS/ZnS core/shell/shell

QDs–KMnO<sub>4</sub> system were recorded. As shown in Fig. 6B, the UV–Vis absorption spectrum of NAC-capped CdTe/CdS/ZnS core/shell/shell QDs–KMnO<sub>4</sub> system and the add absorption spectrum between NAC-capped CdTe/CdS/ZnS core/shell/shell QDs and KMnO<sub>4</sub> could not be superposed within the experimental error, indicating the ground state recombination between NAC-capped CdTe/CdS/ZnS core/shell/shell QDs and KMnO<sub>4</sub>. Furthermore, in comparing with the absorption spectra of NAC-capped CdTe/CdS/ZnS core/shell/shell QDs, the difference absorption spectrum between NAC-capped CdTe/CdS/ZnS core/shell/shell QDs–KMnO<sub>4</sub> system and KMnO<sub>4</sub> exhibited an obvious hypochromic effect. These results reconfirmed to the quenching mechanism of static quenching mechanism attributed to the ground state recombination between NAC-capped CdTe/CdS/ZnS core/shell/shell QDs and KMnO<sub>4</sub>.

#### 4. Conclusions

A novel NAC-capped CdTe/CdS/ZnS core/shell/shell QDs-based “OFF-ON” fluorescent biosensor was established to detect L-ascorbic acid in this paper. The primary advantage of this method is its sensitivity and specificity. The fluorescence of NAC-capped CdTe/CdS/ZnS core/shell/shell QDs could be quenched by KMnO<sub>4</sub> through electron transfer process and the fluorescence of QDs into “OFF” status correspondingly. Then, the fluorescence of QDs could be “ON” after the addition of L-ascorbic acid which could bind with KMnO<sub>4</sub> and take KMnO<sub>4</sub> away from the surface of QDs. Under the optimum conditions, the present method had a linear range of  $8.0 \times 10^{-9}$  M ~  $1.0 \times 10^{-7}$  M, with a correlation coefficient of 0.9971. The limit of detection of L-ascorbic acid was  $1.8 \times 10^{-9}$  M. Some common ions, carbohydrates, nucleotides and amino acids could not infect the L-ascorbic acid determination. The presented method has been applied to the determination of L-ascorbic acid in three synthetic samples, human urine samples and vitamin C tablets successfully. The possible fluorescence quenching mechanism of this NAC-capped CdTe/CdS/ZnS core/shell/shell QDs-based “OFF-ON” fluorescent sensor was the static quenching mechanism.

#### Acknowledgements

This work was financially supported by the National Natural Science Foundation of China (21203035, 21403039), the Guangxi Natural Science Foundation (2013GXNSFCA019005,

2013GXNSFBA019029), the Scientific Research Foundation of Guangxi Provincial Education Department (2013YB138, ZD2014081), the Scientific Research Foundation for the Returned Overseas Chinese Scholars, State Education Ministry, the Open Research Fund Program of the State Key Laboratory of Virology of China (2014KF006) and the Innovation Project of Guangxi Graduate Education (YCSZ2014186).

## References

- [1] M. F. Frasco and N. Chaniotakis, Semiconductor quantum dots in chemical sensors and biosensors, *Sensors*, 2009, **9**, 7266–7286.
- [2] I. L. Medintz, H. T. Uyeda, E. R. Goldman and H. Mattoussi, Quantum dot bioconjugates for imaging, labelling and sensing, *Nat. Mater.*, 2005, **4**, 435–446.
- [3] R. Freeman, R. Gill, I. Shweky, M. Kotler, U. Banin and I. Willner, Biosensing and probing of intracellular metabolic pathways by NADH-sensitive quantum dots, *Angew. Chem. Int. Ed.*, 2009, **48**, 309–313.
- [4] R. Z. Liang, R. Tian, W. Y. Shi, Z. H. Liu, D. P. Yan, M. Wei, D. G. Evans and X. Duan, A temperature sensor based on CdTe quantum dots-layered double hydroxide ultrathin films via layer-by-layer assembly, *Chem. Commun.*, 2013, **49**, 969–971.
- [5] G. W. Platt, F. Damin, M. J. Swann, I. Metton, G. Skorski, M. Cretich and M. Chiari, Allergen immobilisation and signal amplification by quantum dots for use in a biosensor assay of IgE in serum, *Biosens. Bioelectron.*, 2014, **52**, 82–88.
- [6] W. J. Liang, Z. Q. Liu, S. P. Liu, J. D. Yang and Y. Q. He, A novel surface modification strategy of CdTe/CdS QDs and its application for sensitive detection of ctDNA, *Sensor. Actuat. B-Chem.*, 2014, **196**, 336–344.
- [7] T. Yu, T. Y. Ying, Y. Y. Song, Y. J. Li, F. H. Wu, X. Q. Dong and J. S. Shen, A highly sensitive sensing system based on photoluminescent quantum dots for highly toxic organophosphorus compounds, *RSC Adv.*, 2014, **4**, 8321–8327.
- [8] X. Y. Cao, F. Shen, M. W. Zhang, J. X. Bie, X. Liu, Y. L. Luo, J. J. Guo and C. Y. Sun, Facile synthesis of chitosan-capped ZnS quantum dots as an eco-friendly fluorescence sensor for rapid determination of bisphenol A in water and plastic samples, *RSC Adv.*, 2014, **4**, 16597–16606.

- [9] S. Huang, Q. Xiao, R. Li, H. L. Guan, J. Liu, X. R. Liu, Z. K. He and Y. Liu, A simple and sensitive method for L-cysteine detection based on the fluorescence intensity increment of quantum dots, *Anal. Chim. Acta*, 2009, **645**, 73–78.
- [10] M. H. Wang, W. F. Niu, X. Wu, L. X. Li, J. Yang, S. M. Shuang and C. Dong, Fluorescence enhancement detection of uric acid based on water-soluble 3-mercaptopropionic acid-capped core/shell ZnS:Cu/ZnS, *RSC Adv.*, 2014, **4**, 25183–25188.
- [11] D. W. Huang, C. G. Niu, X. Y. Wang, X. X. Lv and G. M. Zeng, “Turn-on” fluorescent sensor for Hg<sup>2+</sup> based on single-stranded DNA functionalized Mn:CdS/ZnS quantum dots and gold nanoparticles by time-gated mode, *Anal. Chem.*, 2013, **85**, 1164–1170.
- [12] F. X. Wang, Z. Y. Gu, W. Lei, W. J. Wang, X. F. Xia and Q. L. Hao, Graphene quantum dots as a fluorescent sensing platform for highly efficient detection of copper(II) ions, *Sensor. Actuat. B-Chem.*, 2014, **190**, 516–522.
- [13] X. Y. Hu, K. Zhu, Q. S. Guo, Y. Q. Liu, M. F. Ye and Q. J. Sun, Ligand displacement-induced fluorescence switch of quantum dots for ultrasensitive detection of cadmium ions, *Anal. Chim. Acta*, 2014, **812**, 191–198.
- [14] J. Zong, X. L. Yang, A. Trinchi, S. Hardin, I. Cole, Y. H. Zhu, C. Z. Li, T. Muster and G. Wei, Carbon dots as fluorescent probes for “off-on” detection of Cu<sup>2+</sup> and l-cysteine in aqueous solution, *Biosens. Bioelectro.*, 2014, **51**, 330–335.
- [15] Y. P. Shi, Y. Pan, H. Zhang, Z. M. Zhang, M. J. Li, C. Q. Yi and M. S. Yang, A dual-mode nanosensor based on carbon quantum dots and gold nanoparticles for discriminative detection of glutathione in human plasma, *Biosens. Bioelectro.*, 2014, **56**, 39–45.
- [16] Z. P. Liu, Q. Ma, X. Y. Wang, Z. H. Lin, H. Zhang, L. L. Liu and X. G. Su, A novel fluorescent nanosensor for detection of heparin and heparinase based on CuInS<sub>2</sub> quantum dots, *Biosens. Bioelectron.*, 2014, **54**, 617–622.
- [17] E. Vaishnavi and R. Renganathan, “Turn-on-off-on” fluorescence switching of quantum dots–cationic porphyrin nano hybrid: a sensor for DNA, *Analyst*, 2014, **139**, 225–234.
- [18] R. Zhang, D. X. Zhao, H. G. Ding, Y. X. Huang, H. Z. Zhong and H. Y. Xie, Sensitive single-color fluorescence “off-on” switch system for dsDNA detection based on quantum dots-ruthenium assembling dyads, *Biosens. Bioelectron.*, 2014, **56**, 51–57.
- [19] S. Huang, H. N. Qiu, Q. Xiao, C. S. Huang, W. Su and B. Q. Hu, A simple QD-FRET

- bioprobe for sensitive and specific detection of hepatitis B virus DNA, *J. Fluoresc.*, 2013, **23**, 1089–1098.
- [20] S. Huang, Q. Xiao, Z. K. He, Y. Liu, P. Tinnefeld, X. R. Su and X. N. Peng, A high sensitive and specific QDs FRET bioprobe for MNase, *Chem. Commun.*, 2008, **44**, 5990–5992.
- [21] P. P. Li, S. P. Liu, S. G. Yan, X. Q. Fan and Y. Q. He, A sensitive sensor for anthraquinone anticancer drugs and hsDNA based on CdTe/CdS quantum dots fluorescence reversible control, *Colloids Surf. A*, 2011, **392**, 7–15.
- [22] Z. Q. Liu, S. P. Liu, X. D. Wang, P. P. Li and Y. Q. He, A novel quantum dots-based OFF–ON fluorescent biosensor for highly selective and sensitive detection of double-strand DNA, *Sensor. Actuat. B-Chem.*, 2013, **176**, 1147–1153.
- [23] R. F. Cathcart, A unique function for ascorbate. *Med. Hypotheses.*, 1991, **35**, 32–37.
- [24] S. J. Padayatty, A. Katz, Y. Wang, P. Eck, O. Kwon, J. H. Lee and S. Chen, Vitamin C as an antioxidant: evaluation of its role in disease prevention, *J. Am. Coll. Nutr.*, 2003, **22**, 18–35.
- [25] P. Janda, J. Weber, L. Dunsch and A. B. P. Lever, Detection of ascorbic acid using a carbon fiber microelectrode coated with cobalt tetramethylpyridopyrroazine, *Anal. Chem.*, 1996, **68**, 960–965.
- [26] O. Arrigori and C. D. Tullio, Ascorbic acid: much more than just an antioxidant, *Biochim. Biophys. Acta*, 2002, **1569**, 1–3.
- [27] L. K. Massey, M. Liebman and S. A. Kynast-Gales, Ascorbate increases human oxaluria and kidney stone risk, *J. Nutr.*, 2005, **135**, 1673–1677.
- [28] B. Mudabuka, D. Ondigo, S. Degni, S. Vilakazi and N. Torto, A colorimetric probe for ascorbic acid based on copper-gold nanoparticles in electrospun nylon, *Microchim. Acta*, 2014, **181**, 395–401.
- [29] T. N. Shekhovtsova, S. V. Muginova, J. A. Luchinina and A. Z. Galimova, Enzymatic methods in food analysis: determination of ascorbic acid, *Anal. Chim. Acta*, 2006, **573-574**, 125–132.
- [30] T. Madrakian, E. Haghshenas and A. Afkhami, Simultaneous determination of tyrosine, acetaminophen and ascorbic acid using gold nanoparticles/multiwalled carbon nanotube/glassy carbon electrode by differential pulse voltammetric method, *Sensor. Actuat. B-Chem.*, 2014, **193**, 451–460.

- [31] H. Chen, R. B. Li, L. Lin, G. S. Guo and J. M. Lin, Determination of L-ascorbic acid in human serum by chemiluminescence based on hydrogen peroxide–sodium hydrogen carbonate–CdSe/CdS quantum dots system, *Talanta*, 2010, **81**, 1688–1696.
- [32] Y. F. Zhang, B. X. Li and C. L. Xu, Visual detection of ascorbic acid *via* alkyne–azide click reaction using gold nanoparticles as a colorimetric probe, *Analyst*, 2010, **135**, 1579–1584.
- [33] G. Q. Wang, Z. P. Chen and L. X. Chen, Mesoporous silica-coated gold nanorods: towards sensitive colorimetric sensing of ascorbic acid *via* target-induced silver overcoating, *Nanoscale*, 2011, **3**, 1756–1759.
- [34] X. X. Wang, J. M. Liu, S. L. Jiang, L. Jiao, L. P. Lin, M. L. Cui, X. Y. Zhang, L. H. Zhang and Z. Y. Zheng, Non-aggregation colorimetric sensor for detecting vitamin C based on surface plasmon resonance of gold nanorods, *Sensor. Actuat. B-Chem.*, 2013, **182**, 205–210.
- [35] W. Bian, J. Ma, W. R. Guo, D. T. Lu, M. Fan, Y. L. Wei, Y. F. Li, S. M. Shuang and M. M. F. Choi, Phosphorescence detection of L-ascorbic acid with surface-attached *N*-acetyl-L-cysteine and L-cysteine Mn doped ZnS quantum dots, *Talanta*, 2013, **116**, 794–800.
- [36] F. Khosravi and H. Asadollahzadeh, Determination of ascorbic acid in different citrus fruits under reversed phase conditions with UPLC, *Euro. J. Exp. Bio.*, 2014, **4**, 91–94.
- [37] Y. J. Chen and X. P. Yan, Chemical redox modulation of the surface chemistry of CdTe quantum dots for probing ascorbic acid in biological fluids, *Small*, 2009, **5**, 2012–2018.
- [38] Q. Xiao, S. Huang, W. Su, W. H. Chan and Y. Liu, Facile synthesis and characterization of highly fluorescent and biocompatible *N*-acetyl-L-cysteine capped CdTe/CdS/ZnS core/shell/shell quantum dots in aqueous phase, *Nanotechnology*, 2012, **23**, 495717.
- [39] A. M. Pisoschi, A. Pop, A. I. Serban and C. Fafaneata, Electrochemical methods for ascorbic acid determination, *Electrochim. Acta*, 2014, **121**, 443–460.
- [40] W. W. Yu, L. H. Qu, W. Z. Guo and X. G. Peng, Experimental determination of the extinction coefficient of CdTe, CdSe, and CdS nanocrystals, *Chem. Mater.*, 2003, **15**, 2854–2860.
- [41] J. N. Demas and G. A. Crosby, The measurement of photoluminescence quantum yields, *J. Phys. Chem.*, 1971, **75**, 991–1024.
- [42] S. Huang, Q. Xiao, W. Su, P. Y. Li, J. Q. Ma and Z. K. He, Simple and sensitive determination of papain by resonance light-scattering with CdSe quantum dots, *Colloids Surf. B*, 2013, **102**,

146–151.

- [43] J. R. Lakowicz, *Principles of Fluorescence Spectroscopy*, 3rd ed, Plenum Press, New York, 2006, pp. 277.
- [44] Y. Chen and Z. Rosenzweig, Luminescent CdS quantum dots as selective ion probes, *Anal. Chem.*, 2002, **74**, 5132–5138.
- [45] N. Shao, Y. Zhang, S. M. Cheung, R. H. Yang, W. H. Chan, T. Mo, K. A. Li and F. Liu, Copper ion-selective fluorescent sensor based on the inner filter effect using a spiropyran derivative, *Anal. Chem.*, 2005, **77**, 7294–7303.
- [46] M. Zheng, Z. G. Xie, D. Qu, D. Li, P. Du, X. B. Jing and Z. C. Sun, On–Off–On fluorescent carbon dot nanosensor for recognition of chromium(VI) and ascorbic acid based on the inner filter effect, *ACS Appl. Mater. Interfaces*, 2013, **5**, 13242–13247.
- [47] Q. Xiao, S. Huang, Z. D. Qi, B. Zhou, Z. K. He and Y. Liu, Conformation, thermodynamics and stoichiometry of HSA adsorbed to colloidal CdSe/ZnS quantum dots, *BBA-Proteins Proteom.*, 2008, **1784**, 1020–1027.

Table 1. Comparison of methods for the determination of L-ascorbic acid

Table 2. Effect of coexisting foreign substances (n = 5)<sup>a</sup>

Table 3. Determination of L-ascorbic acid in three synthetic samples (n = 5)<sup>a</sup>

Table 4. Determination of L-ascorbic acid in human urine samples (n = 5)<sup>a</sup>

Table 5. Detection of L-ascorbic acid in vitamins C tablet (n = 5)<sup>a</sup>

## Figure Captions

Scheme 1. Principle of L-ascorbic acid determination using NAC-capped CdTe/CdS/ZnS core/shell/shell QDs-based “OFF-ON” fluorescent sensor.

Fig. 1. Normalized UV–Vis absorption (a) and fluorescence (b) spectra of NAC-capped CdTe/CdS/ZnS core/shell/shell QDs at room temperature. Insert: Photograph of emission color of NAC-capped CdTe/CdS/ZnS core/shell/shell QDs under the white lamp (Left) and the radiation of UV lamp (Right).

Fig. 2. (A) Fluorescence spectra of NAC-capped CdTe/CdS/ZnS core/shell/shell QDs at different concentrations of  $\text{KMnO}_4$  in Tris-HCl buffer (1.5 mL, pH 7.4). NAC-capped CdTe/CdS/ZnS core/shell/shell QDs:  $1.7 \times 10^{-7}$  M.  $\text{KMnO}_4$ : (a) 0; (b)  $1.7 \times 10^{-6}$  M; (c)  $2.3 \times 10^{-6}$  M; (d)  $3.0 \times 10^{-6}$  M. (B) Fluorescence spectra of NAC-capped CdTe/CdS/ZnS core/shell/shell QDs alone (a), NAC-capped CdTe/CdS/ZnS core/shell/shell QDs with  $1.0 \times 10^{-6}$  M L-ascorbic acid (e), and NAC-capped CdTe/CdS/ZnS core/shell/shell QDs– $\text{KMnO}_4$  system with different concentrations of L-ascorbic acid. NAC-capped CdTe/CdS/ZnS core/shell/shell QDs:  $1.7 \times 10^{-7}$  M;  $\text{KMnO}_4$ :  $3.0 \times 10^{-6}$  M; L-ascorbic acid: (b)  $8.0 \times 10^{-8}$  M; (c)  $5.0 \times 10^{-7}$  M; (d)  $1.0 \times 10^{-6}$  M.

Fig. 3. The influences of pH value (A), buffer volume (B) and QDs volume (C) on the fluorescence intensity response of the system. (A) NAC-capped CdTe/CdS/ZnS core/shell/shell QDs:  $1.7 \times 10^{-7}$  M;  $\text{KMnO}_4$ :  $3.0 \times 10^{-6}$  M; L-ascorbic acid:  $1.0 \times 10^{-7}$  M; Buffer: 1.5 mL Tris-HCl buffer. (B) NAC-capped CdTe/CdS/ZnS core/shell/shell QDs:  $1.7 \times 10^{-7}$  M;  $\text{KMnO}_4$ :  $3.0 \times 10^{-6}$  M; L-ascorbic acid:  $1.0 \times 10^{-7}$  M; Buffer: pH 7.4 Tris-HCl buffer. (C)  $\text{KMnO}_4$ :  $3.0 \times 10^{-6}$  M; Buffer: 1.5 mL Tris-HCl buffer (pH 7.4).

Fig. 4. The influences of  $\text{KMnO}_4$  concentration on the fluorescence intensity response of the system in Tris-HCl buffer (1.5 mL, pH 7.4). NAC-capped CdTe/CdS/ZnS core/shell/shell QDs:  $1.7 \times 10^{-7}$  M.  $\text{KMnO}_4$ : (a) 0; (b)  $2.0 \times 10^{-8}$  M; (c)  $8.0 \times 10^{-8}$  M; (d)  $1.7 \times 10^{-7}$  M; (e)  $3.3 \times 10^{-7}$  M; (f)  $6.7 \times 10^{-7}$  M; (g)  $1.0 \times 10^{-6}$  M; (h)  $1.3 \times 10^{-6}$  M; (i)  $1.7 \times 10^{-6}$  M; (j)  $2.0 \times 10^{-6}$  M; (k)  $2.3 \times 10^{-6}$  M; (l)  $2.7 \times 10^{-6}$  M; (m)  $3.0 \times 10^{-6}$  M. The insert was the linear relationship between  $I_0 / I$  and  $\text{KMnO}_4$  concentration in the range of  $2.0 \times 10^{-8}$  M to  $1.7 \times 10^{-6}$  M with a correlation coefficient of 0.9918.

Fig. 5. Fluorescence spectra of NAC-capped CdTe/CdS/ZnS core/shell/shell QDs and NAC-capped CdTe/CdS/ZnS core/shell/shell QDs– $\text{KMnO}_4$  system with different concentrations of L-ascorbic acid: (a)  $8.0 \times 10^{-9}$  M; (b)  $1.2 \times 10^{-8}$  M; (c)  $2.0 \times 10^{-8}$  M; (d)  $4.0 \times 10^{-8}$  M; (e)  $6.0 \times 10^{-8}$  M; (f)  $1.0 \times 10^{-7}$  M; (g)  $3.0 \times 10^{-7}$  M; (h)  $7.5 \times 10^{-7}$  M; (i)  $1.0 \times 10^{-6}$  M; (j)  $1.5 \times 10^{-6}$  M. The insert was the linear relationship between  $I - I_0$  and L-ascorbic acid concentration in the range of  $8.0 \times 10^{-9}$  M to  $1.0 \times 10^{-7}$  M with a correlation coefficient of 0.9971. NAC-capped CdTe/CdS/ZnS core/shell/shell QDs:  $1.7 \times 10^{-7}$  M;  $\text{KMnO}_4$ :  $3.0 \times 10^{-6}$  M.

Fig. 6. (A) UV–Vis absorption spectrum of  $\text{KMnO}_4$  (a) and the emission spectrum of NAC-capped CdTe/CdS/ZnS core/shell/shell QDs at 388 nm excitation wavelength (b). (B) UV–Vis absorption spectra of NAC-capped CdTe/CdS/ZnS core/shell/shell QDs,  $\text{KMnO}_4$  and NAC-capped CdTe/CdS/ZnS core/shell/shell QDs– $\text{KMnO}_4$  system; the difference absorption spectra between NAC-capped CdTe/CdS/ZnS core/shell/shell QDs– $\text{KMnO}_4$  system and NAC-capped CdTe/CdS/ZnS core/shell/shell QDs, and the add absorption spectrum between NAC-capped CdTe/CdS/ZnS core/shell/shell QDs and  $\text{KMnO}_4$ , respectively. NAC-capped CdTe/CdS/ZnS core/shell/shell QDs:  $8.5 \times 10^{-7}$  M;  $\text{KMnO}_4$ :  $6.0 \times 10^{-6}$  M.

Table 1. Comparison of methods for the determination of L-ascorbic acid

Detection method	Linear range ( $\times 10^{-6}$ M)	Detection limit ( $\times 10^{-6}$ M)	Samples detection	Reference
Spectrophotometry	0.1 ~ 1000000	0.1	Fruit juices, urine, serum, vitamin C tablets	28
Enzymatic analysis	0.1 ~ 10	0.1	Milk and sour-milk products	29
Electroanalysis	1 ~ 150	0.76	Blood serum and pharmaceutical samples	30
Chemiluminescence	0.1 ~ 100	0.0067	Human serum	31
Colorimetry	0.044 ~ 0.3	0.003	Orange juice and grapefruit juice	32
Colorimetry	0.1 ~ 2.5	0.049	Not given	33
Colorimetry	0.11 ~ 85	0.019	Human urine	34
Phosphorimetry	2.5 ~ 37.5	0.72	Human urine	35
Liquid chromatography	Not given	1.1	Citrus fruits	36
Fluorimetry	0.3 ~ 10	0.074	Human urine and plasma	37
Fluorimetry	0.008 ~ 0.1	0.0018	Human urine and vitamin C tablets	This method

Table 2. Effect of coexisting foreign substances (n = 5)<sup>a</sup>

Foreign substances	Concentration coexisting (M)	Change of FL Intensity (%)	R.S.D. (%)	Foreign substances	Concentration coexisting (M)	Change of FL Intensity (%)	R.S.D. (%)
K <sup>+</sup>	5 × 10 <sup>-4</sup>	-2.8	1.4	L-Arg	2 × 10 <sup>-5</sup>	-2.4	1.1
Na <sup>+</sup>	1 × 10 <sup>-3</sup>	-2.1	0.9	L-Cys	1 × 10 <sup>-5</sup>	-2.8	0.7
Ca <sup>2+</sup>	2 × 10 <sup>-4</sup>	+1.6	0.5	L-Val	2 × 10 <sup>-5</sup>	+1.4	0.6
Mg <sup>2+</sup>	5 × 10 <sup>-4</sup>	-2.1	2.7	L-Ala	2 × 10 <sup>-5</sup>	+2.6	2.1
Cu <sup>2+</sup>	1 × 10 <sup>-4</sup>	-1.2	0.8	L-Gly	2 × 10 <sup>-5</sup>	-3.3	0.9
Al <sup>3+</sup>	3 × 10 <sup>-4</sup>	+1.6	1.9	L-Lys	2 × 10 <sup>-5</sup>	+4.2	1.3
C <sub>2</sub> O <sub>4</sub> <sup>2-</sup>	2 × 10 <sup>-4</sup>	+1.1	0.9	L-Trp	2 × 10 <sup>-5</sup>	+3.6	1.8
NO <sub>3</sub> <sup>-</sup>	5 × 10 <sup>-4</sup>	-2.9	1.6	L-Asp	2 × 10 <sup>-5</sup>	-2.6	1.2
SO <sub>4</sub> <sup>2-</sup>	1 × 10 <sup>-4</sup>	-2.8	1.8	L-Pro	2 × 10 <sup>-5</sup>	+1.8	1.5
Cl <sup>-</sup>	1 × 10 <sup>-3</sup>	+1.1	2.5	L-Leu	2 × 10 <sup>-5</sup>	-2.2	2.7
Glucose	1 × 10 <sup>-3</sup>	-2.2	1.1	L-Glu	2 × 10 <sup>-5</sup>	-4.4	1.5
Sucrose	5 × 10 <sup>-4</sup>	-3.1	2.3	L-Tyr	2 × 10 <sup>-5</sup>	+4.9	2.1
Lactose	2 × 10 <sup>-4</sup>	+2.7	0.9	L-Met	2 × 10 <sup>-5</sup>	-3.6	0.7
Urea	5 × 10 <sup>-4</sup>	+2.3	1.3	L-Ser	2 × 10 <sup>-5</sup>	+1.7	1.7
Adenine	2 × 10 <sup>-5</sup>	-3.9	1.2	L-Phe	2 × 10 <sup>-5</sup>	-3.5	1.5
Cytosine	2 × 10 <sup>-5</sup>	-2.7	1.5	L-Thr	2 × 10 <sup>-5</sup>	-3.1	1.9
Thymine	1 × 10 <sup>-5</sup>	-3.9	2.2	L-His	2 × 10 <sup>-5</sup>	-2.4	2.1
Guanine	1 × 10 <sup>-5</sup>	-1.5	1.0	L-Ile	2 × 10 <sup>-5</sup>	+1.8	1.7
L-Asn	2 × 10 <sup>-5</sup>	+1.8	2.8	L-Gln	2 × 10 <sup>-5</sup>	-2.6	2.2

<sup>a</sup> NAC-capped CdTe/CdS/ZnS core/shell/shell QDs: 1.7 × 10<sup>-7</sup> M; KMnO<sub>4</sub>: 3.0 × 10<sup>-6</sup> M; L-ascorbic acid: 3.0 × 10<sup>-7</sup> M; Buffer: 1.5 mL Tris-HCl buffer (pH 7.4).

Table 3. Determination of L-ascorbic acid in three synthetic samples (n = 5)<sup>a</sup>

Synthetic samples	Taken ( $\times 10^{-7}$ M)	Found ( $\times 10^{-7}$ M)	Recovery (%)	R.S.D. (%)
Sample 1 <sup>b</sup>	1.5	1.52 $\pm$ 0.03	101.3	1.4
Sample 2 <sup>c</sup>	5.0	5.01 $\pm$ 0.02	100.2	1.8
Sample 3 <sup>d</sup>	8.0	7.91 $\pm$ 0.05	98.9	1.2

<sup>a</sup> NAC-capped CdTe/CdS/ZnS core/shell/shell QDs:  $1.7 \times 10^{-7}$  M;  $\text{KMnO}_4$ :  $3.0 \times 10^{-6}$  M; Buffer: 1.5 mL Tris-HCl buffer (pH 7.4).

<sup>b</sup> The concentrations of twenty amino acids were all  $1.0 \times 10^{-5}$  M.

<sup>c</sup> The concentrations of glucose, sucrose, lactose and urea were all  $2.0 \times 10^{-4}$  M. The concentrations of adenine, cytosine, thymine and guanine were all  $1.0 \times 10^{-5}$  M.

<sup>d</sup> The concentrations of  $\text{KNO}_3$ ,  $\text{NaNO}_3$ ,  $\text{Ca}(\text{C}_2\text{O}_4)_2$ ,  $\text{Mg}(\text{NO}_3)_2$ ,  $\text{Al}(\text{NO}_3)_3$ ,  $\text{CuSO}_4$  were all  $1.0 \times 10^{-4}$  M.

Table 4. Determination of L-ascorbic acid in human urines (n = 5)<sup>a</sup>

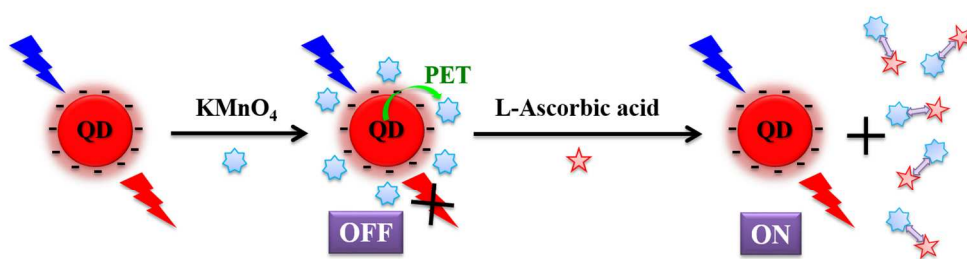
Samples	Taken ( $\times 10^{-8}$ M)	Found ( $\times 10^{-8}$ M)	Recovery (%)	R.S.D. (%)
Human urine sample 1	0.0	5.12 $\pm$ 0.05	–	–
	2.0	7.21 $\pm$ 0.04	104.5	2.0
	5.0	10.10 $\pm$ 0.12	99.6	2.4
	8.0	12.81 $\pm$ 0.08	96.1	1.0
Human urine sample 2	0.0	6.91 $\pm$ 0.01	–	–
	2.0	8.94 $\pm$ 0.05	102.0	2.5
	5.0	12.05 $\pm$ 0.09	103.0	1.8
	8.0	14.82 $\pm$ 0.15	99.0	1.9
Human urine sample 3	0.0	3.12 $\pm$ 0.04	–	–
	2.0	5.11 $\pm$ 0.05	100.5	2.5
	5.0	7.92 $\pm$ 0.10	96.4	2.0
	8.0	10.82 $\pm$ 0.18	96.5	2.3
Human urine sample 4	0.0	9.81 $\pm$ 0.03	–	–
	2.0	11.85 $\pm$ 0.06	102.5	3.0
	5.0	14.71 $\pm$ 0.12	98.2	2.4
	8.0	17.93 $\pm$ 0.21	101.6	2.6
Human urine sample 5	0.0	2.44 $\pm$ 0.12	–	–
	2.0	4.47 $\pm$ 0.05	103.5	2.5
	5.0	7.18 $\pm$ 0.18	95.6	3.6
	8.0	10.75 $\pm$ 0.19	104.4	2.4

<sup>a</sup> NAC-capped CdTe/CdS/ZnS core/shell/shell QDs:  $1.7 \times 10^{-7}$  M;  $\text{KMnO}_4$ :  $3.0 \times 10^{-6}$  M; Buffer: 1.5 mL Tris-HCl buffer (pH 7.4).

Table 5. Detection of L-ascorbic acid in vitamins C tablet (n = 5)<sup>a</sup>

Sample	Taken ( $\times 10^{-8}$ M)	Found ( $\times 10^{-8}$ M)	Recovery (%)	R.S.D. (%)
Vitamins C tablet	0.0	$24.10 \pm 0.82$	–	–
	1.0	$25.12 \pm 0.03$	102.0	3.0
	4.0	$27.92 \pm 0.11$	95.5	2.7
	8.0	$32.35 \pm 0.21$	103.1	2.6

<sup>a</sup> NAC-capped CdTe/CdS/ZnS core/shell/shell QDs:  $1.7 \times 10^{-7}$  M;  $\text{KMnO}_4$ :  $3.0 \times 10^{-6}$  M; Buffer: 1.5 mL Tris-HCl buffer (pH 7.4).



Scheme 1. Principle of L-ascorbic acid determination using NAC-capped CdTe/CdS/ZnS core/shell/shell QDs-based "OFF-ON" fluorescent sensor.  
262x76mm (150 x 150 DPI)

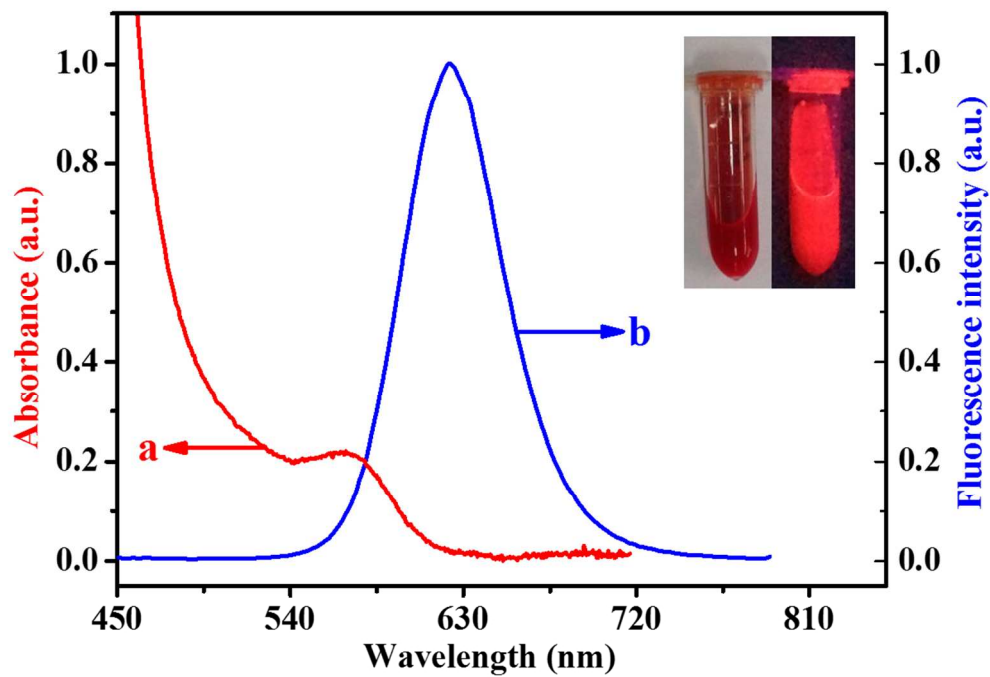


Fig. 1. Normalized UV-Vis absorption (a) and fluorescence (b) spectra of NAC-capped CdTe/CdS/ZnS core/shell/shell QDs at room temperature. Insert: Photograph of emission color of NAC-capped CdTe/CdS/ZnS core/shell/shell QDs under the white lamp (Left) and the radiation of UV lamp (Right).  
204x142mm (150 x 150 DPI)

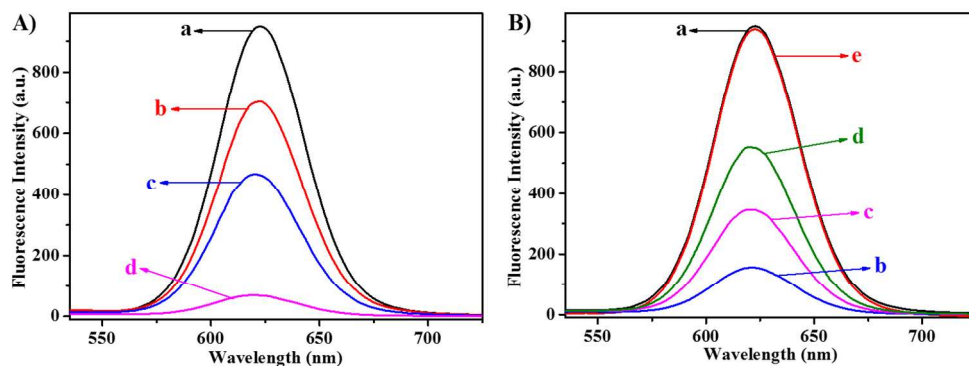


Fig. 2. (A) Fluorescence spectra of NAC-capped CdTe/CdS/ZnS core/shell/shell QDs at different concentrations of KMnO<sub>4</sub> in Tris-HCl buffer (1.5 mL, pH 7.4). NAC-capped CdTe/CdS/ZnS core/shell/shell QDs:  $1.7 \times 10^{-7}$  M. KMnO<sub>4</sub>: (a) 0; (b)  $1.7 \times 10^{-6}$  M; (c)  $2.3 \times 10^{-6}$  M; (d)  $3.0 \times 10^{-6}$  M. (B) Fluorescence spectra of NAC-capped CdTe/CdS/ZnS core/shell/shell QDs alone (a), NAC-capped CdTe/CdS/ZnS core/shell/shell QDs with  $1.0 \times 10^{-6}$  M L-ascorbic acid (e), and NAC-capped CdTe/CdS/ZnS core/shell/shell QDs–KMnO<sub>4</sub> system with different concentrations of L-ascorbic acid. NAC-capped CdTe/CdS/ZnS core/shell/shell QDs:  $1.7 \times 10^{-7}$  M; KMnO<sub>4</sub>:  $3.0 \times 10^{-6}$  M; L-ascorbic acid: (b)  $8.0 \times 10^{-8}$  M; (c)  $5.0 \times 10^{-7}$  M; (d)  $1.0 \times 10^{-6}$  M.

257x98mm (150 x 150 DPI)

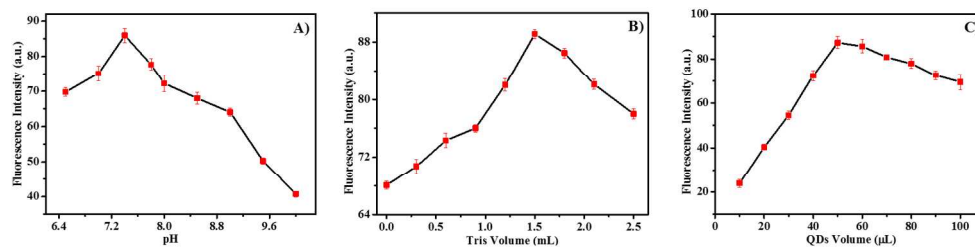


Fig. 3. The influences of pH value (A), buffer volume (B) and QDs volume (C) on the fluorescence intensity response of the system. (A) NAC-capped CdTe/CdS/ZnS core/shell/shell QDs:  $1.7 \times 10^{-7}$  M;  $\text{KMnO}_4$ :  $3.0 \times 10^{-6}$  M; L-ascorbic acid:  $1.0 \times 10^{-7}$  M; Buffer: 1.5 mL Tris-HCl buffer. (B) NAC-capped CdTe/CdS/ZnS core/shell/shell QDs:  $1.7 \times 10^{-7}$  M;  $\text{KMnO}_4$ :  $3.0 \times 10^{-6}$  M; L-ascorbic acid:  $1.0 \times 10^{-7}$  M; Buffer: pH 7.4 Tris-HCl buffer. (C)  $\text{KMnO}_4$ :  $3.0 \times 10^{-6}$  M; Buffer: 1.5 mL Tris-HCl buffer (pH 7.4).  
298x88mm (150 x 150 DPI)

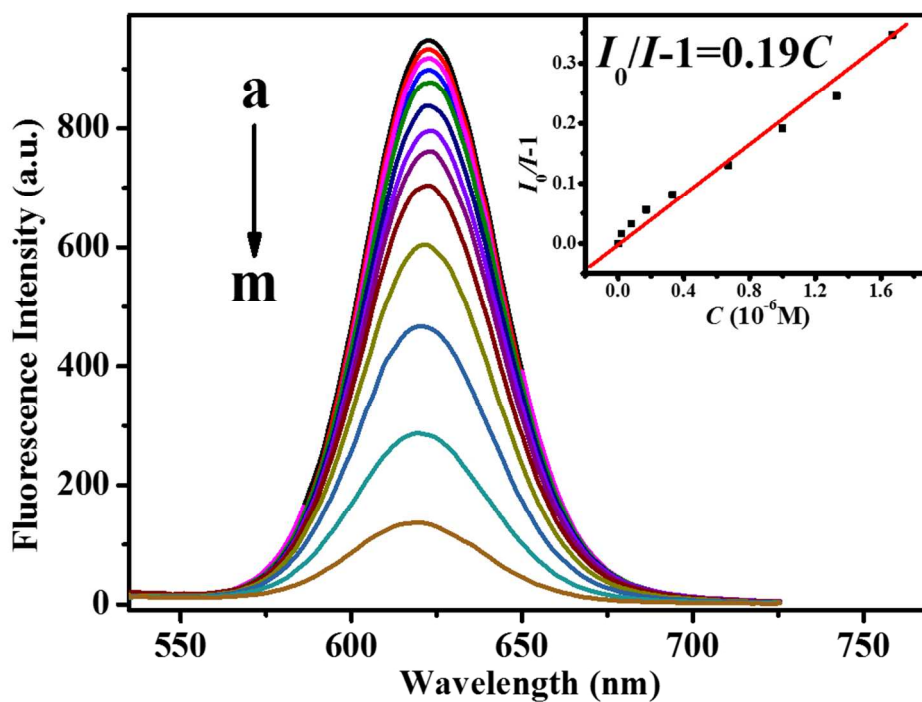


Fig. 4. The influences of KMnO<sub>4</sub> concentration on the fluorescence intensity response of the system in Tris-HCl buffer (1.5 mL, pH 7.4). NAC-capped CdTe/CdS/ZnS core/shell/shell QDs:  $1.7 \times 10^{-7}$  M. KMnO<sub>4</sub>: (a) 0; (b)  $2.0 \times 10^{-8}$  M; (c)  $8.0 \times 10^{-8}$  M; (d)  $1.7 \times 10^{-7}$  M; (e)  $3.3 \times 10^{-7}$  M; (f)  $6.7 \times 10^{-7}$  M; (g)  $1.0 \times 10^{-6}$  M; (h)  $1.3 \times 10^{-6}$  M; (i)  $1.7 \times 10^{-6}$  M; (j)  $2.0 \times 10^{-6}$  M; (k)  $2.3 \times 10^{-6}$  M; (l)  $2.7 \times 10^{-6}$  M; (m)  $3.0 \times 10^{-6}$  M. The insert was the linear relationship between  $I_0 / I - 1$  and KMnO<sub>4</sub> concentration in the range of  $2.0 \times 10^{-8}$  M to  $1.7 \times 10^{-6}$  M with a correlation coefficient of 0.9918.

188x138mm (150 x 150 DPI)

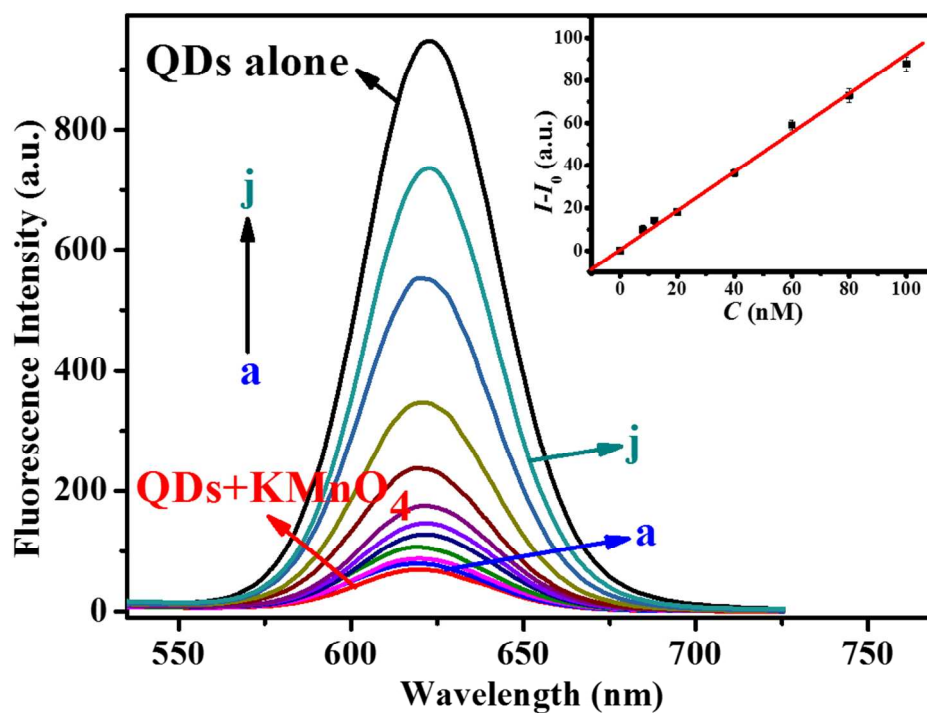


Fig. 5. Fluorescence spectra of NAC-capped CdTe/CdS/ZnS core/shell/shell QDs and NAC-capped CdTe/CdS/ZnS core/shell/shell QDs-KMnO<sub>4</sub> system with different concentrations of L-ascorbic acid: (a)  $8.0 \times 10^{-9}$  M; (b)  $1.2 \times 10^{-8}$  M; (c)  $2.0 \times 10^{-8}$  M; (d)  $4.0 \times 10^{-8}$  M; (e)  $6.0 \times 10^{-8}$  M; (f)  $1.0 \times 10^{-7}$  M; (g)  $3.0 \times 10^{-7}$  M; (h)  $7.5 \times 10^{-7}$  M; (i)  $1.0 \times 10^{-6}$  M; (j)  $1.5 \times 10^{-6}$  M. The insert was the linear relationship between  $I / I_0$  and L-ascorbic acid concentration in the range of  $8.0 \times 10^{-9}$  M to  $1.0 \times 10^{-7}$  M with a correlation coefficient of 0.9971. NAC-capped CdTe/CdS/ZnS core/shell/shell QDs:  $1.7 \times 10^{-7}$  M; KMnO<sub>4</sub>:  $3.0 \times 10^{-6}$  M.  
193x146mm (150 x 150 DPI)

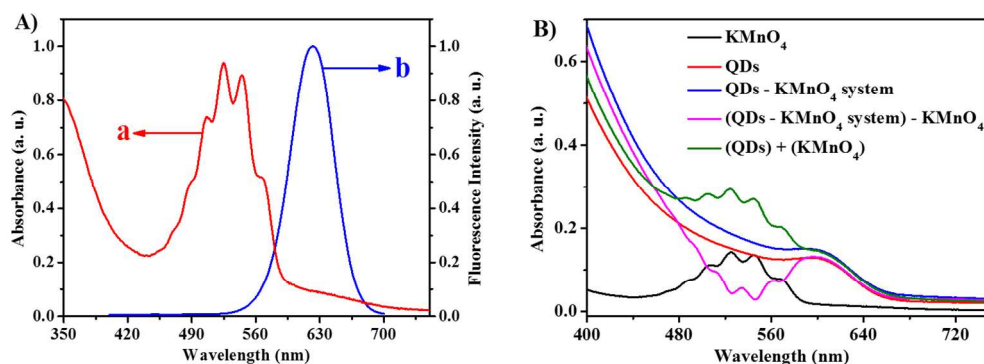


Fig. 6. (A) UV-Vis absorption spectrum of KMnO<sub>4</sub> (a) and the emission spectrum of NAC-capped CdTe/CdS/ZnS core/shell/shell QDs at 388 nm excitation wavelength (b). (B) UV-Vis absorption spectra of NAC-capped CdTe/CdS/ZnS core/shell/shell QDs, KMnO<sub>4</sub> and NAC-capped CdTe/CdS/ZnS core/shell/shell QDs-KMnO<sub>4</sub> system; the difference absorption spectra between NAC-capped CdTe/CdS/ZnS core/shell/shell QDs-KMnO<sub>4</sub> system and NAC-capped CdTe/CdS/ZnS core/shell/shell QDs, and the add absorption spectrum between NAC-capped CdTe/CdS/ZnS core/shell/shell QDs and KMnO<sub>4</sub>, respectively. NAC-capped CdTe/CdS/ZnS core/shell/shell QDs:  $8.5 \times 10^{-7}$  M; KMnO<sub>4</sub>:  $6.0 \times 10^{-6}$  M.  
255x96mm (150 x 150 DPI)